Front. Struct. Civ. Eng. 2022, 16(1): 57–74
https://doi.org/10.1007/s11709-021-0784-y

RESEARCH ARTICLE

Comparative seismic design optimization of spatial steel dome structures through three recent metaheuristic algorithms

Serdar CARBAS[a*], Musa ARTAR[b]

[a] *Department of Civil Engineering, Karamanoglu Mehmetbey University, Karaman 70200, Turkey*
[b] *Department of Civil Engineering, Bayburt University, Bayburt 69000, Turkey*
[*] *Corresponding author. E-mail: scarbas@kmu.edu.tr*

ABSTRACT Steel dome structures, with their striking structural forms, take a place among the impressive and aesthetic load bearing systems featuring large internal spaces without internal columns. In this paper, the seismic design optimization of spatial steel dome structures is achieved through three recent metaheuristic algorithms that are water strider (WS), grey wolf (GW), and brain storm optimization (BSO). The structural elements of the domes are treated as design variables collected in member groups. The structural stress and stability limitations are enforced by ASD-AISC provisions. Also, the displacement restrictions are considered in design procedure. The metaheuristic algorithms are encoded in MATLAB interacting with SAP2000 for gathering structural reactions through open application programming interface (OAPI). The optimum spatial steel dome designs achieved by proposed WS, GW, and BSO algorithms are compared with respect to solution accuracy, convergence rates, and reliability, utilizing three real-size design examples for considering both the previously reported optimum design results obtained by classical metaheuristic algorithms and a gradient descent-based hyperband optimization (HBO) algorithm.

KEYWORDS steel dome optimization, water strider algorithm, grey wolf algorithm, brain storm optimization algorithm, hyperband optimization algorithm

1 Introduction

Throughout history, engineers and designers have always paid special attention to structural systems that allow covering large spaces without any internal support. The issue of how spacious structures can be built has been an influential concept in the development of structural engineering. Additionally, with the increase in demand for structures where activities will take place in parallel with rising population, the need for structural engineering solutions that respond to both aesthetic and economic concerns have arisen. Stadiums, meeting halls, exhibition areas, swimming pools, shopping malls and industrial buildings are typical examples of the structures that demand open and wide spaces and require minimal support inside. As a result of the developments in material and building technologies, steel dome structures have offered advantageous tools in terms of lightness, economy and stability to the structural opportunities available to engineers and designers.

Since steel dome structures are light, rigid and have a high degree of indeterminacy, the structure is not affected as a whole in terms of rupturing under the tension or buckling under the compression that may occur in any bar element in the structural system. Having a high degree of indeterminacy gives advantage to steel dome structures in terms of ensuring a continuous load distribution within the structure. Structural elements of a steel dome are exposed to both axial forces and bending moments that directly affect their axial stiffness due to slenderness [1,2].

A number of recent studies are available in the literature investigating the structural characteristics of steel dome structures from different technical points of

Article history: Received Jul 11, 2021; Accepted Sep 30, 2021

views [3–9]. Also, latterly there have been a variety of attempts made to investigate and examine the optimum design of steel dome structures via metaheuristic algorithms from different aspects [10–20]. Additionally, various studies regarding the analysis of steel dome structures under seismic effects have been conducted [21–30].

As can be seen in the recent studies mentioned above, the optimum designs of steel domes using metaheuristic methods and the analysis of their structural behavior under seismic effects have been carried out separately, covering many distinct perspectives. However, as a result of detailed searches in the literature, no study and/or paper has been found to achieve the structural provision-based optimum designs of spatial steel dome structures under consideration of seismic load effects with new generation nature-inspired metaheuristic algorithms. Thus, the principal goal of this paper is to optimally design the spatial steel dome structures under consideration of seismic load effects utilizing three nature-inspired metaheuristic algorithms. So, it is a promoter study and a pioneer in literature in this respect. The stress and stability design constraints are implemented from ASD-AISC (Allowable Stress Design Code of American Institute of Steel Institution) [31] practice code provisions, and also the displacement constraints are engaged. As optimizer tools, the standard water strider (WS) [32], grey wolf (GW) [33], and brain storm optimization (BSO) [34] algorithms are used to accomplish the solution of optimum steel dome design problems. Furthermore, the optimization process needs seismic responses from structural analysis under external loading conditions which is enabled by open application programming (OAPI) ability of MATLAB [35] through the agency of SAP2000 [36]. Three design examples as of real-size steel dome structures to be designed for minimum weight are considered in order to exhibit the algorithmic performance ability of the proposed metaheuristic algorithms in solving seismic design optimization spatial steel dome problems. More than that, the obtained optimal spatial steel dome structures with minimum design weights via proposed novel WS, GW, and BSO metaheuristic algorithms are compared and evaluated with those that have already been reported in the literature for so-called classical old-fashioned metaheuristic algorithms such as HS, GA, SA and also a gradient descent-based hyperband optimization (HBO) algorithm.

The rest of the sections in this paper are coordinated as the following. Section 2 contains the ASD-AISC provisions based on mathematical expression of design problems for the steel domes. Section 3 surveys the utilization of novel WS, GW, and BSO algorithms. The seismic loading and OAPI are defined in Section 4. And, the achieved optimum structural designs are discussed and explained in Section 5 throughout the design examples. Finally, Section 6 is devoted to the concluding remarks.

2 Design optimization problem definitions and mathematical statements of steel domes structures according to ASD-AISC

In order to minimize the structural weight of the spatial steel dome structures, the design optimization problem can be defined as the following:

$$\min W = \sum_{k=1}^{ng} A_k \sum_{i=1}^{nk} \rho_i L_i, \tag{1}$$

where W denotes bridge weight, A_k represents the areas of cross-sections in the kth member group, density and length of a member i are identified by ρ_i and L_i, respectively, the total numbers of member group is ng, and the total number of members in kth group is nk.

$$\varphi(x) = W(x)\left(1 + P\sum_{i=1}^{m} c_i\right), \tag{2}$$

where the penalty constant is P, the penalized objective function is $\varphi(x)$, and the violated constraint is c_i. The violated constraint can be calculated as follows:

$$g_i(x)\begin{cases} > 0 \rightarrow c_i = g_i(x), \\ \leqslant 0 \rightarrow c_i = 0. \end{cases} \tag{3}$$

The steel dome structures treated as design examples in this study are exposed to the traditional stress and displacement constraints applied in regard to practice codes of ASD-AISC [31] specifications.

The stress constraints are described as the following:

$$g_m = \frac{\sigma_m}{\sigma_{m,\text{all}}} - 1.0 \leqslant 0.0,\ m = 1,\ldots,ne, \tag{4}$$

where σ_m and $\sigma_{m,\text{all}}$ are the calculated and the permitted axial stress values for mth structural element of a steel dome.

The stress constraints for members in tension and compression taken from AISC-AISC are indicated, as the following.

i) The permitted stress is defined for members in tension,

$$\sigma_{\text{t,all}} = 0.6F_{\text{y}}, \tag{5}$$

where the yield stress is denoted as F_{y}.

ii) The permitted stress is expressed for the members in compression,

$$\sigma_{c,all} = \frac{\left[1 - \frac{\lambda_m^2}{2C_c^2}\right] F_y}{\left[\frac{5}{3} + \frac{3\lambda_m}{8C_c} + \frac{\lambda_m^3}{8C_c^3}\right]} \text{ for inelastic buckling } (\lambda_m \geqslant C_c), \tag{6}$$

$$\sigma_{c,all} = \frac{12\pi^2 E}{\lambda_m^2} \text{ for elastic buckling } (\lambda_m < C_c), \tag{7}$$

where $\lambda_m = (K_m L_m)/r_m$ for $m = 1,\ldots,ne$ and $C_c = [(2\pi^2 E)/F_y]^{1/2}$. λ_m exhibits the slenderness ratio, K_m is the effective length factor and taken as 1.0 for structural elements of a steel dome, the r_m is minimal value of radii of gyration, and C_c is parameter of crucial slenderness ratio.

Additionally, the displacement constraints can be stated as the following:

$$g_j = \frac{\delta_{jl}}{\delta_{ju}} - 1.0 \leqslant 0.0, \; j = 1,\ldots,n, \tag{8}$$

where δ_{jl} is displacement of jth degree of freedom, δ_{ju} is upper limit of displacement, n is number of limited displacements.

3 Metaheuristic algorithms

For years, the engineers, researchers, and practitioners have sought creative optimization techniques to investigate the optimum solutions of complicated design problems in various engineering branches including structural and civil engineering problems [37–42]. For decreasing the computational cost of the optimum design procedures, some surrogate models integrated with recent optimization algorithms have also been proposed and improved by the researchers and applied to broad range of engineering fields [43–47].

In this study, the standard versions of WS [32], GW [33], BSO [34] algorithms, which are recent vintage metaheuristic algorithms, are introduced to seismic design optimization of spatial steel dome structures. The main reason for choosing these three algorithms as optimizer tools is that all three algorithms have very easy and practical solution improvisation functions. Moreover, they have few algorithmic parameters and thus all of them have fast convergence rate. Besides, as well as having simple principles, the rapid search space, the search accuracy, and the ease of application to practical engineering design problems are the common advantages of WS, GW, and BSO algorithms. Also, the implementation of these algorithms to the structural design optimization problems such as spatial steel dome designs is scarce in the literature.

3.1 Water strider algorithm

One of the contemporary nature-inspired metaheuristic algorithms imitating the coupling, social life and characteristics of water strider aquatic insects is so-called WS algorithm [32]. The prominent feature that makes the WS algorithm stand out is its influential exploitation and exploration phases. The chief algorithm steps may briefly be marked in following.

1) Initialization. The eggs are stocked by a female water strider from two to twenty days. The water striders lay away their eggs on water sports or on undersea rocks by surrounding them with a very gelatinous-like content. All feasible designs (solutions) are assumed as to be randomly scattered in search space in this algorithm. Thereby, the population can be initially generated by Eq. (9).

$$WS_i^{\text{initial}} = L_b + rand * (U_b - L_b) \; (i = 1,2,...,nws), \tag{9}$$

where the ith water strider primal position is identified by WS_i^{initial} and the lower and the upper bounds of the design variables are represented by L_b and U_b, respectively. An arbitrary random number produced as to be uniformly distributed between [0,1] is *rand*. The *nws* stands for the water strider number. If the amount of available food (water striders' position fitness) is high, then, after generating an initial population from a design pool, obtaining a potentially better objective function is within the bounds of possibility.

2) Establishment of territories. The water striders settle and protect a particular territory where it is admissible to mate and reach an available source of food. For establishing *nt* territories, the water striders are sorted according to their fitness values in the standard WS algorithm. Then, *nws*/*nt* numbers of territory groups are created. Also, the water strider numbers surviving in a territory are kept unchanged and thus every territory is gathered by selecting an individual (water strider) from each group.

3) Mating attitude. In order to provoke the desire for mating, the water is gently ruffled to move a male water strider towards a female. It is not possible to predict how the female water strider reacts to this demand, a 'p probability' that equals 0.5 is identified so that there is an equal chance of acceptance or rejection. So, in standard WS algorithm the Eq. (10) is used to update the male water strider position.

$$\begin{aligned} &\text{if mating accepted (with } p = 0.5), \\ &\qquad WS_i^{\text{new}} = WS_i^{\text{current}} + rand \cdot R, \\ &\text{else} \qquad WS_i^{\text{new}} = WS_i^{\text{current}} + (rand + 1) \cdot R, \end{aligned} \tag{10}$$

where the male water strider's initial location is WS_i^{current} and an arbitrary number generated between [0,1] is *rand*.

The ruffle wave radius, R, presented in Eq. (11) can be expressed as distance from a male water strider's initial position (WS_i^{current}) to the female water strider's position (WS_F^{current}) in same territory.

$$R = WS_{\text{F}}^{\text{current}} - WS_i^{\text{current}}. \tag{11}$$

4) Foraging strategy. The male water strider consumes excessive energy whether mating or not. Thus, at the novel position the male water strider looks for nutrient to satisfy the demand for energy. For this purpose, the existence of nutrient resources should be specified via objective function evaluation. The objective function fitness has to be preferable than the former one so that the male water strider can obtain a source of food at his novel position. The mathematical expression of this situation is given in Eq. (12).

$$WS_i^{\text{new}} = WS_i^{\text{current}} + 2 \cdot rand \cdot (WS_{\text{BL}}^{\text{current}} - WS_i^{\text{current}}), \tag{12}$$

where the $WS_{\text{BL}}^{\text{current}}$ denotes the best water strider position with optimal objective function.

5) Ending of survive and replacement. When a male water strider cannot detect any source of food at his novel position, his life is terminated and he is replaced with a novel one by the aid of formulation given in Eq. (13).

$$WS_i^{\text{new}} = L_{\text{b}_j}^{\text{current}} + rand * (U_{\text{b}_j}^{\text{current}} - L_{\text{b}_j}^{\text{current}}), \tag{13}$$

where the $L_{\text{b}_j}^{\text{current}}$ and $U_{\text{b}_j}^{\text{current}}$ present the lower and upper positions of the water strider in the jth territory.

6) Termination. The algorithm is ended when the predefined termination criterion is reached, signifying the optimum solution. Otherwise, it loops again from the third step and proceeds again for a novel search.

3.2 Grey wolf algorithm

The so-called GW algorithm was originated by imitating community living and hunting strategies of grey wolves in nature [33]. Concerning the community hierarchy of grey wolves, they can be categorized as α (alpha), β (beta), δ (delta), and ω (omega). The wolf community has a dominant alpha and the others obey its rules. Beta is a subordinate individual in the group helping the alpha one in decision making. Delta is the least significant character in the group of grey wolves. Additionally, if any wolf is indefinable as α, β, and/or δ in the group, this individual is titled as omega. The grey wolves conspiratorially interact with each other while they are hunting. The chief algorithm steps are defined below with their fundamental features [33,48].

1) Social hierarchy. The community hierarchy of a wolf group is taken into account to configure the candidate solutions. The obtained solutions are respectively categorized as α, β, δ, and ω wolves in terms of their fitness values from best to worst.

2) Surrounding prey. The fact that grey wolves surround a prey while hunting can be expressed mathematically as in following Eqs. (14) and (15).

$$\vec{D} = \left| \vec{C} \cdot \vec{X}_{\text{p}} - \vec{X}(t) \right|, \tag{14}$$

$$\vec{X}(t+1) = \vec{X}_{\text{p}}(t) - \vec{A} \cdot \vec{D}, \tag{15}$$

where current iteration is t, the coefficient vectors are $\vec{A}$ and $\vec{C}$, and the vector of prey position is $\vec{X}_{\text{p}}$. The $\vec{A}$ and $\vec{C}$ can be calculated by following Eq. (16).

$$\begin{aligned} \vec{A} &= 2 \cdot \vec{a} \cdot \vec{r}_1 - \vec{a}, \\ \vec{C} &= 2 \cdot \vec{r}_2. \end{aligned} \tag{16}$$

where the vector $\vec{a}$ components are linearly declined from 2 to 0 in duration of iterations. The random $\vec{r}_1$ and $\vec{r}_2$ vectors are produced interim of [0,1].

3) Hunting. The α, β, and δ individuals in a grey wolf group have specific data on the prey's current position. Hence, the best three of the solutions acquired are registered so that the others in the group can update their positions accordingly. Mathematically, the Eqs. (17)–(19) are utilized to model this logic.

$$\text{ss}\vec{D}_\alpha = \left| \vec{C}_1 \cdot \vec{X}_\alpha - \vec{X} \right|, \ \vec{D}_\beta = \left| \vec{C}_2 \cdot \vec{X}_\beta - \vec{X} \right|, \ \vec{D}_\delta = \left| \vec{C}_3 \cdot \vec{X}_\delta - \vec{X} \right|, \tag{17}$$

$$\vec{X}_1 = \vec{X}_\alpha - \vec{A}_1 \cdot \vec{D}_\alpha, \ \vec{X}_2 = \vec{X}_\beta - \vec{A}_2 \cdot \vec{D}_\beta, \ \vec{X}_3 = \vec{X}_\delta - \vec{A}_3 \cdot \vec{D}_\delta, \tag{18}$$

$$\vec{X}(t+1) = \frac{\vec{X}_1 + \vec{X}_2 + \vec{X}_3}{3}. \tag{19}$$

4) Lunge to prey. In this step, since the $\vec{a}$ vector value is reduced, the variation range of the vector $\vec{A}$ is also reduced. If the $\vec{A}$ vector is randomly decided between [−1,1], the following search agent position falls anywhere between its own current position and prey position. In other words, if $|A| < 1$, the prey is lunged by grey wolf.

5) Seeking for prey. The positions of α, β, and δ individuals in a group of grey wolves are related to usefulness for seeking a prey. The group individuals disperse to seek a prey and gather again to lunge when they detect a prey. The dispersion of the wolves can be modelled mathematically according to fitness of the $\vec{A}$ vector that is randomly set as greater than 1 or less than –1. So, when $|A| > 1$ then grey wolves are permitted to walk away from prey to search for a more advantageous one. This strategy further advances the widescale search ability of GW algorithm.

6) Stopping. If the predefined criterion of termination is reached, the running of the GW algorithm ceases.

3.3 Brain storm optimization algorithm

The so-called BSO algorithm is a nature-inspired metaheuristic algorithm propounded by simulating a human group activity of brain storming to bring forth enormous ideas for optimal solutions to design problems. In BSO algorithm, the humans possessing various knowledge and experiences gather to constitute a group for discussing the ideas [34]. The humans share their particular ideas to create an idea database. Those ideas are valued with respect to their scale and then clustered in subgroups. Afterwards, novel ideas are reproduced utilizing basic idea database and the experienced information. Those processes proceed till the most acceptable ideas are identified [49]. The fundamental steps of BSO algorithm steps are defined as follows [50–52].

1) Very similarly to formerly described metaheuristics, the initial design generation and the evaluation (numbers of individuals *NI*) are executed at the first step via Eq. (20).

$$X_i = X_{\mathrm{L}} + rand \cdot (X_{\mathrm{U}} - X_{\mathrm{L}}) \ (i = 1, 2, \ldots, NI), \tag{20}$$

where the X_{U} and X_{L} are the maximum and minimum limits of design variables.

2) The initial attained designs are clustered in subgroups by aid of a K-means technique. Then, the attained designs in every cluster are assorted in a descending order in terms of their fitness and the cluster center is interpreted as the best designs in each cluster.

3) The cluster centers are randomly variated according to pre-detected probability that is called P_{s}. And then, on the basis of *NI* (numbers of individual in clusters), the cluster selection probability is computed by Eq. (21).

$$P_{\mathrm{Cl},i} = \frac{NI_i}{NI} \ (i = 1, 2, ..., N_{\mathrm{Cl}}), \tag{21}$$

where the cluster selection probability is denoted as $P_{\mathrm{Cl},i}$ for cluster *i*, and its cluster number is N_{Cl}.

4) In this step the generation of candidate designs is performed. This process is split into two forms. In the first, one cluster is utilized to generate candidate designs. In the latter, two clusters are utilized to generate candidate designs. Which of these forms is used is decided by the following criteria:

If $(rnd < Ps_{4,1})$ **Then**
The candidate design is produced utilizing one cluster.
Else
The candidate design is produced utilizing two clusters.
Endif (22)

where the $Ps_{4,1}$ is previously detected probability utilized for choosing a cluster to produce novel design.

In the lead form, a cluster is randomly chosen in a group. If the P_{Cl} is lower than *rnd* random value, the cluster is eliminated and then a novel cluster is arbitrarily chosen. After cluster choice, the generation of candidate designs is performed as the following:

Randomly select one cluster *j*
If $(rnd < Ps_{4,2})$ **Then**
$x_k^{\mathrm{cand}} = Center_{j,k};\ k = 1, 2, \ldots, ng$
Else (23)
Select any individual $(j1)$ from the cluster *j*
$x_k^{\mathrm{cand}} = X_{i1,k};\ k = 1, 2, \ldots, ng$
Endif

where the $Ps_{4,2}$ is chosen cluster's utilized probability and the *ng* is the number of members of the group.

In the latter form, the two clusters are randomly chosen from the group. Then, the generation of candidate designs is performed as the following:

Randomly select two cluster *j*1 and *j*2
If $(rnd < Ps_{4,2})$ **Then**
$x_j^{\mathrm{cand}} = rnd \cdot Center_{j1,k} + (1 - rnd) * Center_{j2,k};$
$k = 1, 2, \ldots, ng$
Else . (24)
Select any individual $(i1)$ from the cluster *j*1
Select any individual $(i2)$ from the cluster *j*2
$x_k^{\mathrm{cand}} = rnd * X_{i1,k} + (1 - rnd) * X_{i1,k};\ k = 1, 2, \ldots, ng$
Endif

5) In this step, in order to augment diversity, the generation of candidate designs is specified. For this purpose, the step length of *SL* is added to candidate designs. Computation of *SL* and candidate design updating process are expressed as the following:

$$SL = logsig\left((0.5Iter_{\max} - iter)/20\right) \cdot rand, \tag{25}$$

$$x_k^{\mathrm{cand_{new}}} = x_k^{\mathrm{cand_{current}}} + 6 \cdot SL \cdot (rand - 3). \tag{26}$$

After adding *SL*, the greedy selection process by which if new design is better than the previous in terms of design fitness, the previous one is replaced by the new design.

6) The algorithm steps from 2 to 5 are reiterated till a preassigned maximum iteration number is reached.

4 Seismic loading and open application programming interface

In this study, the response spectrum data and graph automatically generated by SAP2000 [36] are demonstrated in Table 1 and Fig. 1, respectively, where the site class C as stated in AASHTO-Table 3.10.3.1-1 [53] is selected for seismic loading for all design examples.

Table 1 Response spectrum data generated by SAP2000

period (s)	acceleration
0	0.954
0.032888	1.399333
0.065776	1.844667
0.098664	2.29
0.493319	2.29
0.6	1.882833
0.8	1.412125
1	11.297
1.2	0.941417
1.4	0.806929
1.6	0.706063
1.8	0.627611
2	0.56485
2.5	0.45188
3	0.376567
3.5	0.322771
4	0.282425
4.5	0.251044
5	0.22594
5.5	0.2054
6	0.188283
6.5	0.1738
7	0.161386
7.5	0.150627
8	0.141213
8.5	0.132906
9	0.125522
9.5	0.118916
10	0.11297

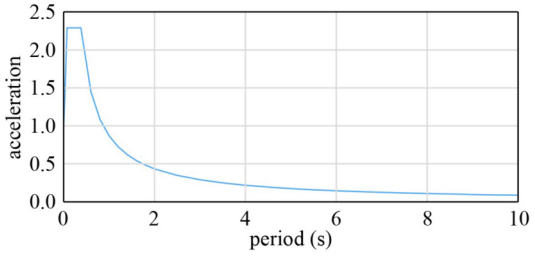

Fig. 1 Response spectrum graph automatically generated by SAP2000.

As stated above, in order to execute the seismic effect and obtain the response spectrum for the dome structures the AASHTO-LRFD practice seismic code provisions are selected. The chief logic to prefer AASHTO_LRFD as the specification of seismic provisions in this study is that automatic description of response spectrum and site class is possible for AASHTO specification without any manual input using SAP2000 software within the policy of OAPI for integration with MATLAB.

Also, in this study, in addition to the load combinations present in the loading conditions of the design examples, a new load combination containing the seismic load effect is added to loading conditions of all design examples as $D + 0.7E_x$ in which D denotes dead load and E_x stands for earthquake load (seismic effect) on global x-direction. In order to obtain the E_x seismic load effect according to AASHTO-LRFD specifications, the detail seismic response spectrum data (Table 2) automatically generated from SAP2000 is utilized basically in accordance with Table 1 and Fig. 1.

Moreover, the structural response of a spatial steel dome structure is needed under external loading conditions including seismic load effect when the cross-sectional features are chosen from the design pool by a metaheuristic algorithm. The SAP2000 structural analysis program is utilized to create structural responses containing a response spectrum for seismic effect and make them available to users by allowing admission through inbuilt functions. These functions, so-called OAPI functions, are in conformity with various coding languages, one of which is MATLAB. The OAPI functions create an interface so that any modelling and analyzing value obtained from one software can be used by any other software. Thus, in this study, the OAPI functions pertaining to the SAP2000 are utilized to create an interface to the optimization algorithms encoded with MATLAB in order to establish the structural responses of steel dome structures to be used in the optimization process. So, thanks to the OAPI, data is transferred between SAP2000 and MATLAB in a safe and accurate manner. The optimum design algorithm encoded in MATLAB begins designating various steel sections for the dome elements in the structural model and then this data is conveyed to SAP2000 via OAPI in order to analyze the steel dome structure under the identified loading combinations. Then, the structural analysis responses, namely internal forces, displacements, stresses, etc., are input into the optimization algorithm to control whether a feasible structure can be established by the designated sections or not. This reciprocal data transferring process is repeated until the predefined termination criterion of the optimization algorithm is reached. The flowchart that summarizes the methodology is demonstrated in Fig. 2.

5 Design examples

The principle aim of this study is to accomplish the optimum design of spatial steel dome structures with

Table 2 Detail data on response spectrum used for generation of seismic load effect

FuncDamp	*Ss*	*S*1	*PGA*	SiteClass	F_a	F_v	F_{pga}	*SDS*	*SD*1
0.05	2.29	0.869	0.954	C	1	1.3	1	2.29	1.1297

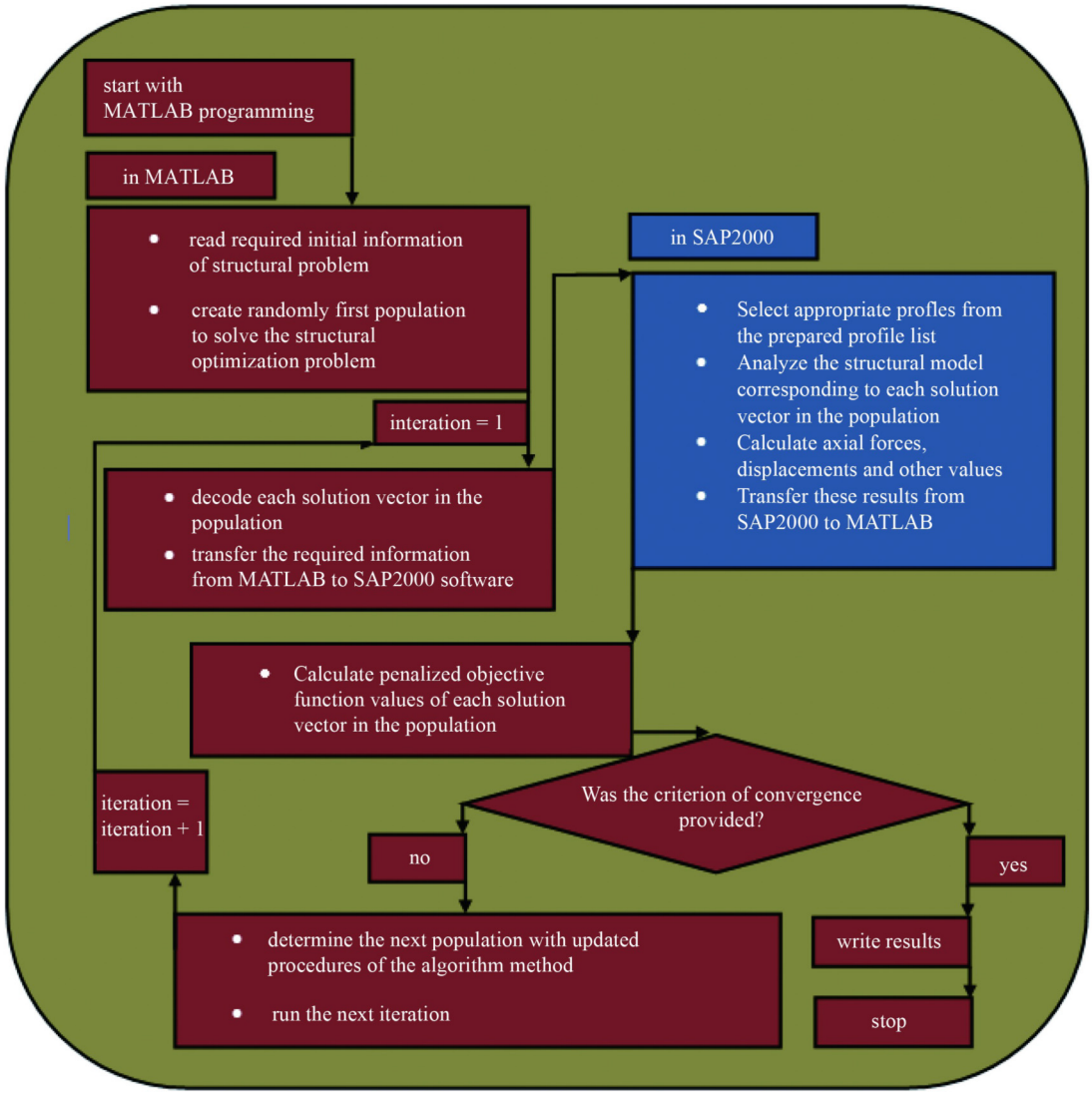

Fig. 2 The flowchart of the methodology.

minimum design weights under seismic load. To do so, the areas of cross-sections of structural elements are handled as design variables selected within allowable range and collected in member groups. For this purpose, three different real-size spatial steel dome structures are employed as design examples of this study. These are 120-bar spatial steel dome, 130-bar spatial steel dome, and 354-bar spatial steel dome structures. All of these have previously been optimally designed without seismic load effect via so-called classical metaheuristic algorithms such as harmony search (HS), genetic algorithm (GA), cascade optimization (CO) for 120-bar spatial steel dome [54–56], simulated annealing (SA), evolutionary strategies (ESs), particle swarm optimization (PSO), tabu search (TS), ant colony optimization (ACO), standard genetic algorithm (SGA) for 130-bar [57] and 354-bar spatial steel dome structures [58]. Besides, the 354-bar spatial steel dome structure has already been optimally designed via the big bang-big crunch (BB-BC) algorithm [59]. However, in design examples, only the results of the methods that produced the best dome design among the classical metaheuristic techniques mentioned above are presented and discussed in order to avoid repetition. For conducting a fair comparison and evaluation on the algorithmic performances (such as convergence rate and accuracy of the proposed contemporary WS algorithm, GW algorithm, and BSO algorithm) all design examples under loading conditions with and without considering seismic load effect are also optimally designed by using HBO algorithm [60]. This is

one of the most up to date gradient descent-based optimization algorithms that iteratively allocate resources to a set of random configurations.

In this study, as stated before, the brand-new WS, GW, and BSO algorithms are utilized as optimizers for achieving the seismic design optimization of steel dome structures considering the displacement constraints as well as the ASD-AISC [31] practice code provisions for stress and stability constraints. Each design example is engaged and interpreted separately whether or not extra load combination containing the seismic (earthquake) effect ($D + 0.7E_x$) is added to the existing loading conditions.

As tabulated in Table 3, the parameter sets considered in the WS, GW, and BSO algorithms are selected conformably with offered values in former resource studies [32–34] in addition to comprehensively operated numerical examinations. Nevertheless, it is well-known that metaheuristic algorithms are sensitive to characteristics of optimum design problem tried to be solved. Thus, it is almost impossible to certainly tune each optimization technique to perform with its best capacity for all design examples taken into account in this study. Every design example that is considered is separately resolved several times (more than 10 times) with each proposed optimization method, ending with dissimilar optimum designs after each execution owing to the probabilistic nature of those optimization methods. Also, the previously described maximum structural analysis number varies for each algorithm utilized in every design example: 200 for 120-bar spatial steel dome, 300 for 130-bar spatial steel dome and 700 for 354-bar spatial steel dome structure. So, the maximum number of iterations, considered as termination criteria of all solution algorithms, is equal to multiplication of the population size and the maximum structural analysis number for each algorithm.

5.1 120-bar spatial steel dome structure

The 120-bar spatial steel dome structure illustrated in Fig. 3 is treated as the first design problem in this study. The 120 bars are collected into seven member groups (Fig. 3(a)), due to the structural symmetry. Modulus of elasticity (E) is 210 GPa and the material density (ρ) is 7971.810 kg/m^3 for all structural members. The yield stress of steel (F_y) is taken as 400 MPa. This spatial steel dome structure was initially examined by Soh and Yang [61] to acquire the optimal sizing and configuration variables, such as the structural configuration optimization.

But, in this study, in order to reach the minimum design weight of the dome, only the design variables that are the steel bars assigned to the member groups are optimized. The loading of the dome is considered to be such that vertical loading acts at all the unsupported joints. These loads are taken as −60 kN at node 1, −30 kN at nodes 2 through 13, and −10 kN at all the other nodes. This is the first loading case in which the seismic effect is not taken into consideration. In this study, $+0.7E_x$ seismic load effect is applied to all unsupported nodes in addition to the just defined dead loads (D), which is described as the second loading case ($D + 0.7E_x$) taken into consideration the seismic effect. The cross-sectional areas of the steel bars designated to the members in the groups are selected among 1 to 129.3 cm^2 so that a section list containing a total number of 119 steel pipe sections is created as a design pool [56]. Beside the stress and stability constraints adopted from ASD-AISC specifications, all nodes of the dome are subjected to the displacement limitation of ±0.5 cm in x-, y-, and z-directions.

Table 3 Set of parameters for each metaheuristic algorithm

algorithm	parameters set
WS	p: 0.5, pop. size: 20
GW	$\vec{a}$: (linearly decline 2 to 0), $\vec{r}_1$ and $\vec{r}_2$: [0, 1], pop. size: 20
BSO	N_{Cl}: 20, P_{S3}: 0.2, $P_{S4,1}$: 0.8, $P_{S4,2}$: 0.4, pop. size: 20

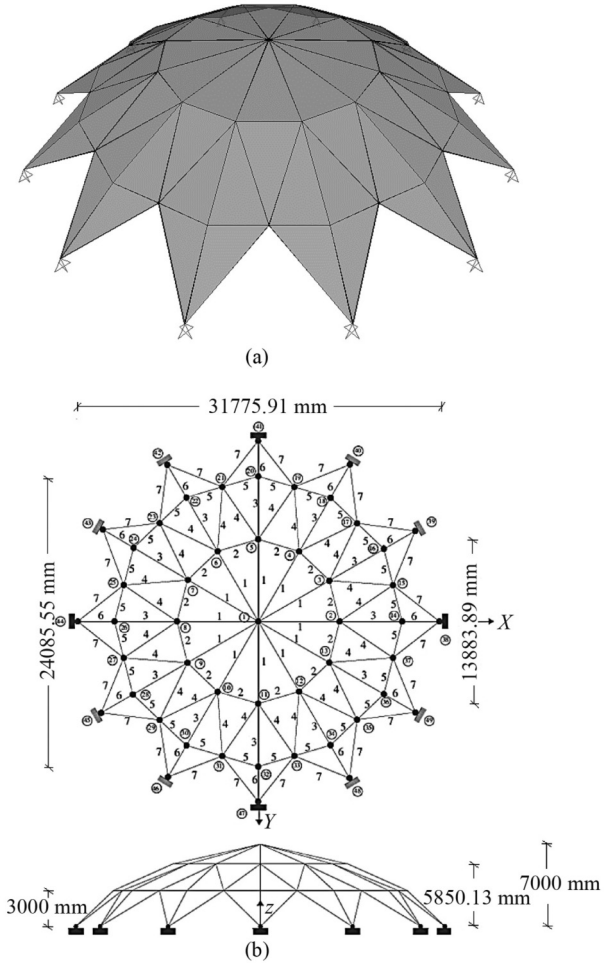

Fig. 3 120-bar spatial steel dome structure. (a) 3D view and (b) plan and elevation views.

For this design example, optimum steel profile areas assigned to the member groups via all solution algorithms are presented in Table 4. Additionally, the optimal steel dome designs with minimum design weights for all solution algorithms and the maximum displacements, maximum stress ratios, and the necessary structural analyses under both loading cases, with and without considering seismic effect for WS, GW, and BSO metaheuristic algorithms and gradient descent-based HBO algorithm, are presented in Table 5. Also, from these tables the currently achieved optimal dome designs with novel metaheuristic and gradient descent-based algorithms are compared with those formerly announced in the literature based on so-called old-fashioned classical metaheuristics for load case where the seismic load effect is not involved.

If the load case without seismic effect is considered, the steel pipe sections acquired via GW algorithm, which is preceded among all other algorithms, yield the lightest dome structures for this design example. The WS and BSO algorithms obtained the second and the third optimum design weight for the same loading conditions as 85.19 and 85.32 kN, respectively. All steel dome structures with novel GW, WS, and BSO algorithms are lighter than those already reported in literature obtained through GA, CO, and HS algorithms [54–56]. Furthermore, the gradient descent-based HBO algorithm yielded the heaviest dome designs for this design example under loading condition without seismic load effect. The GW algorithm generates the optimum design weight of 84.43 kN which is the lightest design for 120-bar spatial steel dome structure and the GW algorithm needs only 126 structural analyses out of 200. The gradient descent-based HBO algorithm yields the optimum dome design at 196 structural analysis that is very close to the maximum number of iterations of 200.

If the seismic load effect is regarded for this design example, once again the GW algorithm outperforms BSO and WS algorithms with design weight of 84.89 kN. But, at this loading condition the second design weight is produced by BSO as 85.42 kN. The WS algorithm accomplishes the design optimization weight of 86.08 kN when seismic load is considered. It is interesting that the optimal steel dome designs achieved by GW, BSO, and WS algorithms under effect of seismic loading are all lighter than those design weight yielded by GA, CO, and HS algorithms where the seismic load effect is not considered. For this loading condition, once again the gradient descent-based HBO algorithm achieved the worst design with the heaviest dome design weight. For this loading condition, it is also worth stating that although the BSO algorithm achieved the second best

Table 4 Optimally selected cross-sectional areas of steel pipe profiles assigned to member groups via solution algorithms for 120-bar spatial steel dome structure

group no.	previously reported studies (cm^2)			this study (cm^2)							
	HS [54]	GA [55]	CO [56]	BSO		GW		WS		HBO	
	I	I	I	I	II	I	II	I	II	I	II
1	21.27	19.48	19.85	21.24	21.24	21.24	21.24	21.24	22.65	26.28	28.32
2	17.99	17.29	40.02	14.45	14.45	14.05	13.77	14.05	13.32	13.77	14.45
3	24.98	10.97	11.48	12.09	12.09	15.61	13.32	14.90	12.09	13.77	14.45
4	16.58	19.48	21.58	18.39	18.97	18.39	18.97	18.97	18.97	18.97	18.97
5	7.41	9.55	10.14	8.63	10.52	8.08	8.29	7.49	10.52	13.32	8.63
6	21.49	14.52	12.53	18.97	13.77	13.77	14.05	14.05	15.61	17.10	16.52
7	17.94	23.74	15.01	22.65	23.26	22.65	23.43	23.26	22.65	23.26	24.76

Notes: I: without seismic load effect, II: with seismic load effect, HS: harmony search, GA: genetic algorithm, CO: cascade optimization, BSO: brain storm optimization, GW: grey wolf, WS: water strider, HBO: hyperband optimization.

Table 5 Obtained optimum designs via solution algorithms for 120-bar spatial steel dome structure

optimum design solutions	previously reported studies (cm^2)			this study (cm^2)							
	HS [54]	GA [55]	CO [56]	BSO		GW		WS		HBO	
	I	I	I	I	II	I	II	I	II	I	II
weight (kN)	88.52	86.83	87.24	85.32	85.42	84.43	84.89	85.19	86.08	92.49	93.19
max. disp. (cm)	–	–	–	0.08	0.06	0.1	0.1	0.1	0.12	0.14	0.15
max. stress ratio	–	–	–	0.99	0.99	0.99	0.99	0.99	0.99	0.88	0.88
needed structural analyses	–	–	–	175	131	126	196	135	175	196	197

Notes: I: without seismic load effect, II: with seismic load effect, HS: harmony search, GA: genetic algorithm, CO: cascade optimization, BSO: brain storm optimization, GW: grey wolf, WS: water strider, HBO: hyperband optimization.

optimum dome weight, after the GW algorithm, it outperformed all other algorithms in terms of computational effort with 131 structural analyses out of 200, while the GW algorithm yielded the optimal dome after 196 structural analyses. Similarly, when the seismic load is considered, the gradient descent-based HBO algorithm demonstrates relatively poor computational effort since it reached the optimum dome design after 197 structural analyses.

Also, for both load cases with and without considering seismic effect, it is apparent from Table 5 that while the displacement constraints achieved with GW, WS, and BSO algorithms are far from its limit value of 0.5 cm, the stress constraints that dominate the optimization process are almost at its upper bound of 1.0. From the same table, however, when the displacement and stress constraints are examined for the gradient descent-based HBO algorithm, it is noticed that the obtained displacement constraint values are far from the limit value in both loading conditions, as is the case for the three proposed metaheuristic algorithms, but the stress constraints do not dominate the optimization process as much.

It can be also ensured from the design history curves exhibited in Figs. 4(a) and 4(b) that the variations of minimum dome weight with iterations carried out by the GW algorithm are less than with WS, BSO, and HBO algorithms for both load cases (without and with seismic load effect). Also, the computational efforts of the all-solution algorithms can easily be observed from these figures for both loading conditions.

In order to illustrate the distribution of optimal designs obtained from novel GW, WS, and BSO algorithms as well as gradient descent-based HBO algorithm, the box plots of each algorithm under consideration, with and without seismic load effect, are depicted in Fig. 5. It is evident from this plot that while the BSO algorithm performs in a very narrow range, the GW, WS, and HBO algorithms perform in wider ranges.

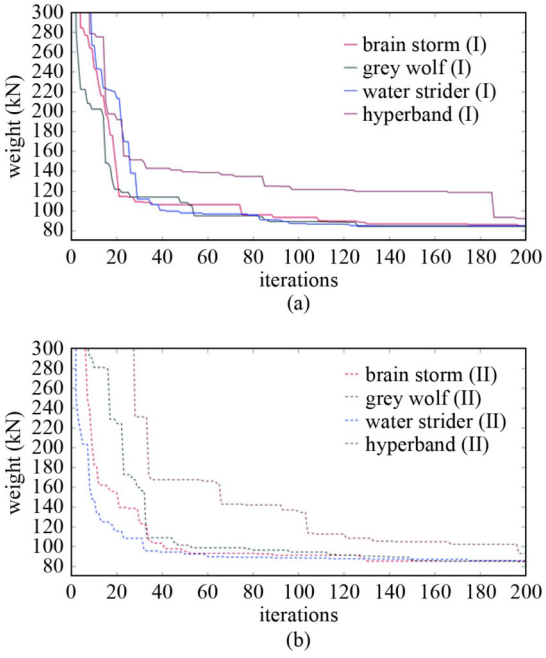

Fig. 4 Design history graphs for 120-bar spatial steel dome structures. (a) Without seismic load effect; (b) with seismic load effect.

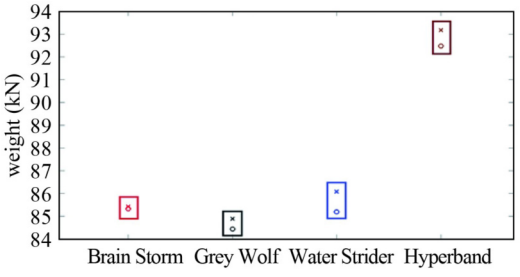

Fig. 5 The box plot of the optimum designs for 120-bar spatial steel dome structure. *o*: solutions without seismic effect, *x*: solutions with seismic effect.

5.2 130-bar spatial steel dome structure

The second design example of this study is conducted as a real size 130-bar spatial steel dome structure. Figure 6 presents 3D, top, and elevation views, of this steel dome having a base diameter of 20 m and a total height of 4 m. This design example comprising 51 nodes and 130 structural members are sorted into 8 groups which are treated as the design variables. The design variables are chosen from an available pipe section list consisting of 37 circular hollow steel sections itemized in ASD-AISC. The stress and stability limitations of the structural members are computed according to the provisions of ASD-AISC, as defined in Section 2. Furthermore, all structural members are restricted in terms of slenderness (λ) where $\lambda \leqslant 300$ for members in tension and $\lambda \leqslant 200$ for members in compression. Also, the maximum displacement value of the nodes in the dome is limited with 2.62 cm in any direction. The modulus of elasticity (E) is taken as 200 GPa and the yield stress (F_y) is taken as 250 MPa [57].

For the design purpose as the first load case, where the seismic effect is not considered in the load conditions, the dome is exposed to a total of eight loading combinations as: (i) $DL + SLB$, (ii) $DL + TP$, (iii) $DL + TN$, (iv) $DL + WEP + WIP$, (v) $DL + WEP + WIN$, (vi) $DL + 0.75\,(WEP + WIP) + 0.75SLB$, (vii) $DL + 0.75\,(WEP + WIN) + 0.75SLB$, (viii) $DL + 0.75TN + 0.75SLB$ where dead load (DL) is 200 Pa, balanced snow load (SLB) is 830 Pa, wind load with positive internal pressure (WIP) is 200 Pa, wind load with negative internal pressure (WIN) is 200 Pa. In order to apply the wind load with external pressure (WEP) to the dome, it is divided into three parts as a windward quarter, a center half and a leeward quarter so

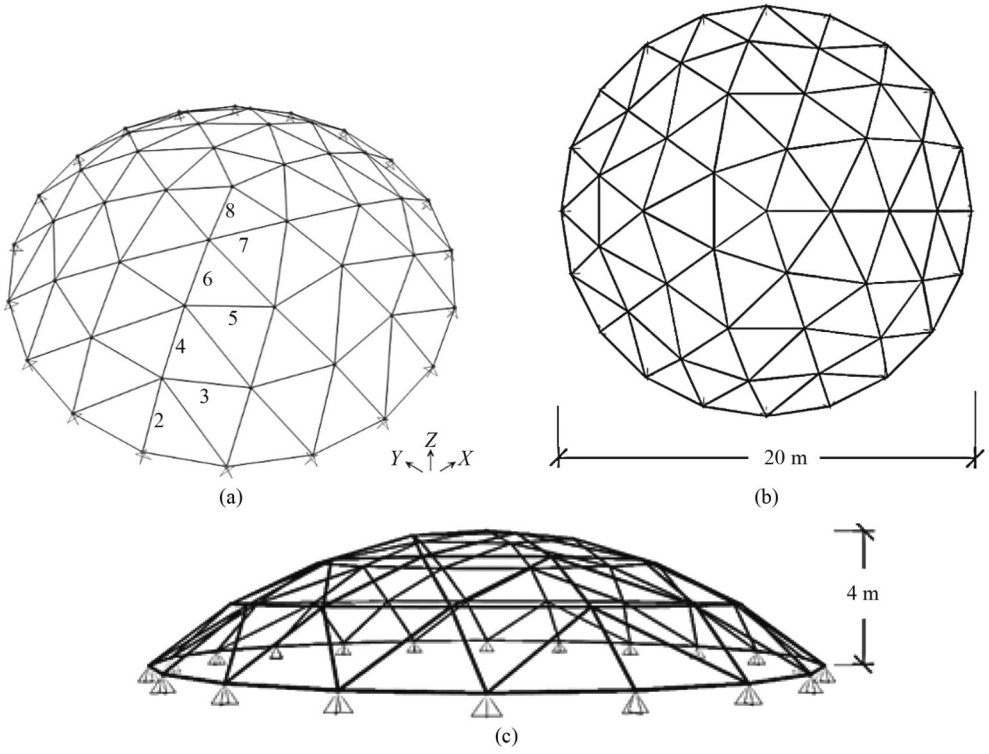

Fig. 6 130-bar spatial steel dome structure. (a) 3D view and member grouping; (b) top view; (c) elevation view.

that *WEP* values on each part are 10, 859, and 473 Pa, respectively. The positive temperature change (*TP*) and negative temperature change (*TN*) are calculated for ±20° change in temperature of entire dome structure. More detailed definitions of the loading conditions of this design example can be found in the source paper reported in literature [57]. Moreover, consistent with the primary aim of this study, when the seismic effect is considered in the loading conditions as a second load case, a ninth loading combination of ($DL + 0.7E_x$) is added to the existing abovementioned eight ones.

In Table 6, the optimally selected steel pipe profiles assigned to member groups via solution algorithms for this design example is tabulated. In the same table, for the load case where the seismic effect is not considered, the optimum dome design previously achieved by the SA algorithm is also presented for a fair evaluation of the algorithmic performances of the proposed novel algorithms. For this purpose, the optimal designs acquired by previously reported SA algorithm and the novel WS, GW, and BSO metaheuristic algorithms and gradient descent-based HBO algorithm for either load cases with and without considering seismic load effect is displayed in Table 7. For the load case where the seismic effect is not considered, the WS, GW, and BSO metaheuristic algorithms and the gradient descent-based HBO algorithm generated the same optimum solution with design weight of 24.2 kN. That is exactly the same as for the design previously reported for the SA algorithm [57]. This solution is displayed in Table 7 and yields the optimal dome design for this design example. For the second load case where the seismic effect is considered, while GW and WS algorithms located the same optimal design as in the first load case, the BSO and HBO algorithms generated heavier dome designs. The dome design produced by BSO and HBO algorithms are 0.83% and 4.55% heavier than those obtained from GW and WS algorithms. For the BSO algorithm the difference is only caused by the steel pipe designation to the eighth member group. For the HBO algorithm, in addition to eighth member group, the steel pipe designations differ also in

Table 6 Optimally selected steel pipe profiles assigned to member groups via solution algorithms for 130-bar spatial steel dome structure

group no.	previously reported study	this study							
	SA [57]	BSO		GW		WS		HBO	
	I	I	II	I	II	I	II	I	II
1	P2.5	P2.5	P2.5	P2.5	P2.5	P2.5	P2.5	P2.5	P2.5
2	P2	P2	P2	P2	P2	P2	P2	P2	P2
3	P2	P2	P2	P2	P2	P2	P2	P2	P2
4	P2	P2	P2	P2	P2	P2	P2	P2	P2
5	P2	P2	P2	P2	P2	P2	P2	P2	PX2
6	P2	P2	P2	P2	P2	P2	P2	P2	P2
7	P2	P2	P2	P2	P2	P2	P2	P2	PX2
8	P1.5	P1.5	PX1.5	P1.5	P1.5	P1.5	P1.5	P1.5	P1.5

Notes: I: without seismic load effect, II: with seismic load effect, SA: simulated annealing, BSO: brain storm optimization, GW: grey wolf, WS: water strider, HBO: hyperband optimization.

Table 7 Obtained optimum designs via solution algorithms for 130-bar spatial steel dome structure

optimum design solutions	previously reported study	this study							
	SA [57]	BSO		GW		WS		HBO	
	I	I	II	I	II	I	II	I	II
weight (kN)	24.2	24.2	24.4	24.2	24.2	24.2	24.2	24.2	25.3
max. disp. (cm)	–	0.60	0.53	0.60	0.60	0.60	0.60	0.6	0.67
max. stress ratio	–	0.76	0.75	0.76	0.76	0.76	0.76	0.76	0.76
max. slenderness ratio; /200 (for comp. mem.); /300 (for tension mem.)	–	0.98	0.98	0.98	0.98	0.98	0.98	0.98	0.98
needed structural analyses	–	218	139	208	159	195	164	291	283

Notes: I: without seismic load effect, II: with seismic load effect, SA: simulated annealing, BSO: brain storm optimization, GW: grey wolf, WS: water strider, HBO: hyperband optimization.

the fifth and the seventh members groups. While the GW and WS algorithms assign P1.5 steel pipe section to the eighth element group and P2 steel pipe section to the fifth and seventh element groups, the BSO and HBO algorithms assign a slightly heavier PX1.5 steel pipe section to the eighth element group and the HBO algorithm assign heavier PX2 steel pipe section to the fifth and the seventh element groups when the seismic load is included in the loading conditions.

It is worth mentioning that, there is a solution in this table on obtained constraint values. Although, both the displacement and stress ratio constraints are far from their mentioned upper bounds the slenderness ratio constraints are almost at their upper bound of 1.0 for both load cases and all metaheuristic and gradient descent-based algorithms. Nevertheless, the slenderness ratio constraint controls the optimization process in all solution algorithms, and the stress ratio constraint also moderately affects the optimization process. Yet, the displacement constraint has hardly any impact on optimization for any algorithm as seen in Table 7. Furthermore, one of the striking results shown from this table concerns the needed structural analyses that show the computational efforts of the proposed solution algorithms. The point to be noted here is that the computational efforts of all solution algorithms under the loading condition, where the seismic effect is not considered, are higher than the load case where the seismic effect is considered. By the way, the worst computational effort is displayed by gradient descent-based HBO algorithm for both loading conditions which are very close to the maximum iteration number of 300 for this design example.

The design history curves of this design example are plotted as shown in Fig. 7 with and without seismic load effect displaying the improvisation of the best feasible dome design based on search operation to identify optimal algorithmic performances of all solution algorithms. From Fig. 7(a) for load case without seismic effect, it can be seen that amongst the solution algorithms the optimum design is converged at nearly similar phases of optimization process by WS and GW; however, the BSO and HBO algorithms identify the optimal dome

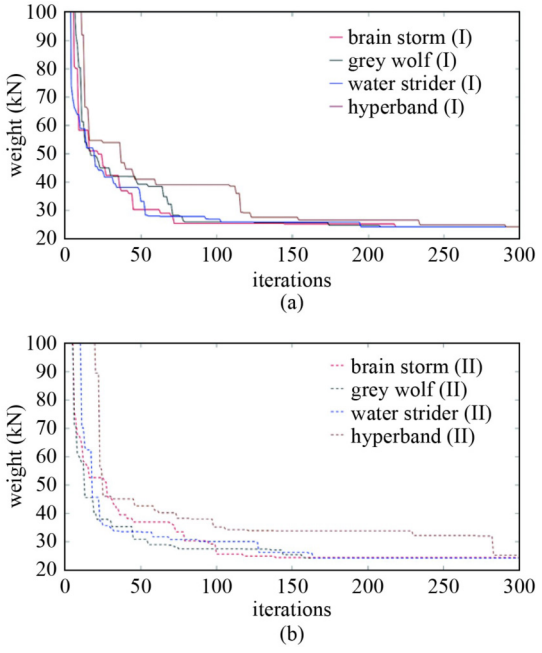

Fig. 7 Design history graphs for 130-bar spatial steel dome structures. (a) Without seismic load effect; (b) with seismic load effect.

design relatively slowly. As can be understood from Fig. 7(b) for load case with seismic load effect, even the BSO shows a rapid convergence in the direction of the optimal design especially in early phases of optimum search; it identifies the optimum design later than WS and GW metaheuristic algorithms with a slightly heavier design weight. From the same figure, it can be deduced that the gradient descent-based HBO algorithm presents course convergence rates in the path of optimum design process and identifies the optimal design very slowly.

The box plots of WS, GW, and BSO metaheuristic algorithms and HBO gradient descent-based algorithm are portrayed in Fig. 8 to show the separation of achieved optimal designs for load cases with and without consideration of seismic load effect. It is evident from the figure that WS and GW algorithms have exactly identical optimum designs for both load cases, exhibiting steady

search features of the algorithms. It can also be noticed that the BSO algorithm has a very narrow range between optimal designs attained for the either load cases. But the HBO algorithm has wider range between obtained optimum designs for both load cases.

5.3 354-bar spatial steel dome structure

The last and the more extreme design example of this study is a 354-bar spatial steel dome structure whose 3D, plan, and elevation views are shown in Fig. 9. This dome structure has 40 m diameter, 8.28 m height, 127 nodes, and 354 structural members. The structural members, namely 354 steel bars, are sorted into 22 independent design variables as member groups. These are chosen from a ready list including 37 circular hollow sections tabulated ASD-AISC. For the load case without considering seismic effect, the dome is structurally analyzed under three different loading cases created as the combinations of dead (D), snow (S) and wind (W) loads and computed in accordance with ASCE 7-10 [62]. The loading combinations acting on the dome are i) $D + S$, ii) $D + S + W$ (with negative internal pressure), and iii) $D + S + W$ (with positive internal pressure). In order to prevent the extra computational demand, the unbalanced snow loads are ignored. So, in this study, it is presumed that while dead and snow loads act on the projected area, the wind load acts on the curved surface area. Dead load pressure is taken as 200 Pa. The design snow load P_s is calculated as 830 Pa. For calculating the design load of wind, the velocity pressure is computed as 1115 Pa and then the design wind pressure is calculated as a combined effect of internal and external pressures acting on the roof. The dome is split up as three fields, windward quarter, center half, and leeward quarter, so that the external wind pressure can be calculated. The final pressure acting on different zones of the dome is achieved by conjoining the internal and external wind pressures as described exhaustively in reference source study [58]. For the second load case, considering seismic effect in load combinations, an additive fourth load combination is acted on the dome structure as $D + 0.7E_x$. The stress and

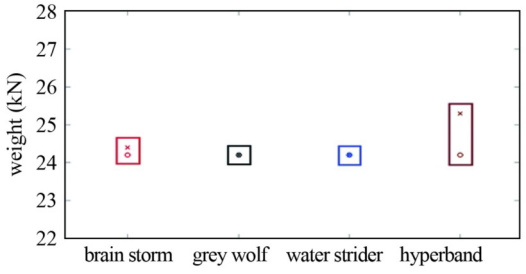

Fig. 8 The box plot of the optimum designs for 130-bar spatial steel dome structure. *o*: solutions without seismic effect, *x*: solutions with seismic effect.

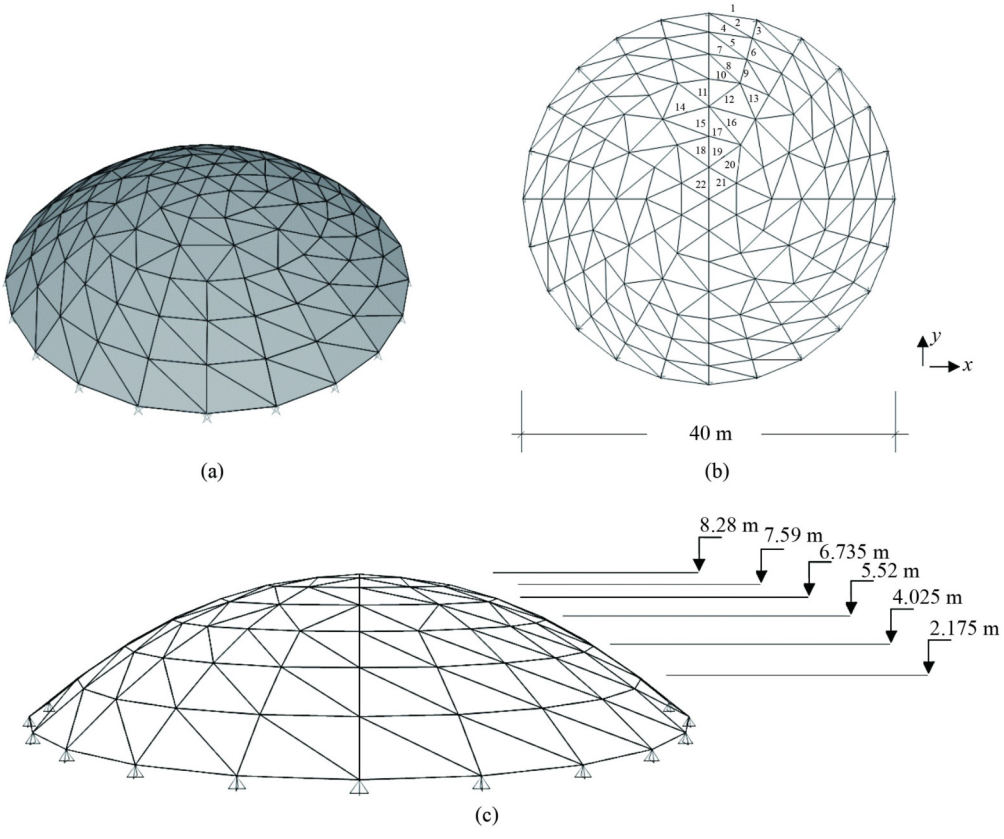

Fig. 9 354-bar spatial steel dome structure. (a) 3D view; (b) top view and member grouping; (c) elevation view.

stability restrictions of structural elements are employed in accordance with the specifications of ASD-AISC. The upper bound of the displacements of all joints is restricted to 11.1 cm in each direction. Moreover, as for the previous design example, all structural members are restrained with respect to slenderness (λ) so that upper value of $\lambda \leqslant 300$ for members in tension and $\lambda \leqslant 200$ for members in compression. The modulus of elasticity (E) is taken as 200 GPa, the yield stress (F_y) is considered as 250 MPa, and the tensile stress (F_u) is taken as 310 MPa.

While the optimum section designations selected to be assigned to member groups via both previously reported SA and BB-BC algorithms and those selected through GW, WS, and BSO metaheuristic algorithms and HBO gradient descent-based algorithm are presented in Table 8. Moreover, the obtained optimum designs through all solution algorithms are tabulated in Table 9. It is apparent from these tables, for load case without seismic effect that the GW algorithm produces the lightest dome design of 144.54 kN. This best feasible dome design is chased by those generated from BSO and WS algorithms having design weight of 147.74 and 152.08 kN, respectively, and the heaviest dome is designed by gradient descent-based HBO algorithm with a 162.42 kN design weight. For this load case it should be underlined that the optimal dome design obtained from the GW algorithm is slightly lighter (0.18%) than the dome design obtained from the SA algorithm, but slightly heavier (0.21%) than the BB-BC algorithm currently available in the literature [58,59]. Similarly, when comparing the dome designs obtained with the BSO and WS algorithms and the already announced dome designs obtained with the SA and BB-BC algorithms, the dome produced by the BSO algorithm is 1.99% and 2.37% heavier than those of the SA and BB-BC algorithms, respectively. Also, the dome design generated by the WS algorithm is 5.02% heavier than those of the SA algorithm and 5.15% heavier than those of the BB-BC algorithm. Finally, the HBO algorithm also produced 12.17% and 12.60% heavier domes than SA and BB-BC algorithms, respectively. Also, for this loading case (without seismic load effect) when only the obtained dome designs via novel proposed solution

Table 8 Optimally selected steel pipe profiles assigned to member groups via solution algorithms for 354-bar spatial steel dome structure

group no.	previously reported studies (cm^2)		this study (cm^2)							
	SA [58]	BB-BC [59]	BSO		GW		WS		HBO	
	I	I	I	II	I	II	I	II	I	II
1	P2	P2	P3	P3	P3	P3	P3	P3	PX4	PX3.5
2	P3	P3.5	P4	P4	P4	P4	P4	P4	P4	PX3.5
3	P4	P3	P3	P3	P3	P3	P3	P3	P3	PX3
4	P3.5	P3	P3.5	P3.5	P3.5	P3.5	P3.5	P3.5	P3.5	P3.5
5	P3	P3	P3	P3	P3	P3	P3.5	P3.5	P3.5	P3.5
6	P3	P3	P3	P3	P3	P3	P3	P3	P3	P3
7	P3	P3.5	P3	P3	P3	P3	P3	P3	P3	P3.5
8	P2.5	P3	P2.5	P2.5	P2.5	P2.5	P2.5	P2.5	P2.5	P2.5
9	P3	P2.5	P2.5	PXX2	P2.5	P2.5	PX2.5	PX2.5	P2.5	PX2.5
10	P3	P3	P2	P2	P2	P2	P2	P2	P2	P2
11	P2.5	P2.5	P2.5	PX2	PX2	PX2	PX2	PX2	PX2	P2.5
12	P2.5	P2.5	P2.5	P2.5	P2.5	PX2.5	P3	P3	P2.5	PX3
13	P2.5	P2.5	PX2.5	P3	P2.5	P2.5	P3	P3	P2.5	P2.5
14	P2.5	P2.5	PX2.5	PX2.5	P2.5	P2.5	P2.5	P2.5	P2.5	P3
15	P2.5	P2.5	P2.5	P2.5	P2.5	P2.5	P2.5	P2.5	P2.5	PXX2
16	P2.5	P2.5	P2.5	P2.5	P2.5	P2.5	P2.5	P2.5	P2.5	P2.5
17	PX2	PX2	PX2	PX2	PX2	PX2	PX2	PX2	PX2	PX2
18	PX2	PX2	P2	P2.5	P2	P2.5	P2	PX2	P2	P3
19	P2	P2	P2	P2	P2	P2	P2	P2	PX2	PX2
20	P2	P2	P2	P3	P2	PX2	P2	P2	P2	P2
21	P2	P2	P2	P2	P2	P2	P2	P2	P3	PX2
22	P2	P2	P2	P2	P2	P2	P2	P2	P2	PX2

Notes: I: without seismic load effect, II: with seismic load effect, SA: simulated annealing, BB-BC: big bang-big crunch, BSO: brain storm optimization, GW: grey wolf, WS: water strider, HBO: hyperband optimization.

Table 9 Obtained optimum designs via solution algorithms for 354-bar spatial steel dome structure

optimum design solutions	previously reported studies (cm^2)		this study (cm^2)							
	SA [58]	BB-BC [59]	BSO		GW		WS		HBO	
	I	I	I	II	I	II	I	II	I	II
min. weight (kN)	144.80	144.24	147.74	152.83	144.54	146.89	152.08	152.44	162.42	176.46
max. disp. (cm)	–	–	1.20	1.17	1.22	1.21	1.18	1.17	0.98	1.08
max. stress ratio	–	–	0.88	0.91	0.94	0.94	0.94	0.94	0.94	0.99
max slend. ratio; /200 (for comp. members) /300 (for tens. members)	–	–	1.00	1.00	1.00	1.00	1.00	1.00	1.00	1.00
needed structural analyses	–	–	673	637	695	626	669	559	583	641

Notes: I: without seismic load effect, II: with seismic load effect, SA: simulated annealing, BB-BC: big bang-big crunch, BSO: brain storm optimization, GW: grey wolf, WS: water strider, HBO: hyperband optimization.

algorithms are compared with each other, the GW algorithm outperforms the BSO, WS, and HBO algorithms.

From Table 9, for the second load case of this design example, as stated before when the seismic load effect is considered among loading combinations, the GW algorithm produces the lightest dome design with 146.89 kN design weight which is followed by WS algorithm with a dome design weight of 152.44 kN. For this second load case, the BSO algorithm produces the dome design with a 152.83 kN design weight. And, the HBO algorithm generates the heaviest dome design with a 176.46 kN for this loading case. Considering these dome designs, the BSO algorithm produced a dome design that is 2.94% lighter than the WS algorithm for the first load case, while the WS algorithm produced a dome design that is 0.26% lighter than the BSO algorithm in the second load case where the seismic load effect was considered.

For both load cases, if the upper bounds of the design constraints are examined from Table 9, it is apparent that the slenderness ratio strongly dominates the optimization process since its obtained values are at its upper bound of 1.0 for all proposed GW, WS, BSO, and HBO algorithms. It is apparent from the same table that although the impact is slightly less than the slenderness ratio constraint, for all solution algorithms the stress constraint plays a significant role in managing the optimum design procedure. It is easily seen from Table 9 that the displacement constraint plays a more passive role in the optimization process than other constraints in this design example since its obtained values are very far from the upper bound for all algorithms.

There is another interesting point that should be seen from Table 9, that when the seismic load effect is not considered in the loading combination, although the gradient descent-based HBO algorithm produced the heaviest dome design, it achieved this design with the least computational effort, as 583 out of 700 structural analyses. Also, it performs with a moderate computational effort that resembles those of GW, WS, and BSO metaheuristic algorithms when seismic load effect is taken in to account in the loading combination. For both load cases, when the computational efforts exhibited by all of the solution algorithms are examined, it is seen that the solution conducted by the GW algorithm without seismic load effect has the worst effort, with 695 out of 700 structural analyses.

The algorithmic performance of the GW, WS, BSO metaheuristic algorithms and HBO gradient descent-based algorithm to identify the optimum dome designs under both load cases during optimization process can be seen from Fig. 10 with respect to with and without seismic load effect. These graphs depict the convergence rates over search records representing the variation of the best feasible attained designs throughout the optimization procedure with respect to the GW, WS, BSO, and HBO algorithms under load combinations with and without considering seismic load effect. For both load cases (with and without considering seismic effect), while the GW algorithm demonstrates better convergence and identifies the optimum designs, the HBO algorithm displays poor convergence characteristics ending with the worst dome designs. Interestingly, it can be concluded from Fig. 10 that despite BSO algorithm illustrating relatively fast convergence performance during early phases of design optimization, its performance deteriorates in the later phases and it eventuates in a worse optimal solution.

In Fig. 11, the box plots revealing the distribution of optimal dome designs of every metaheuristic algorithm are presented for this design example. It is apparent from this figure that the WS algorithm has a restricted interim, showing the constant search features of the algorithm. Also, it can be seen that the GW algorithm and the BSO algorithm have wider interims and the gradient descent-based HBO algorithm has the widest range.

6 Concluding remarks

In this study, the WS algorithm, GW algorithm, and the BSO algorithm are conducted to achieve seismic design optimization of steel dome structures. Also, to display the algorithmic performance capacities of these proposed metaheuristics, in addition to comparison of the obtained

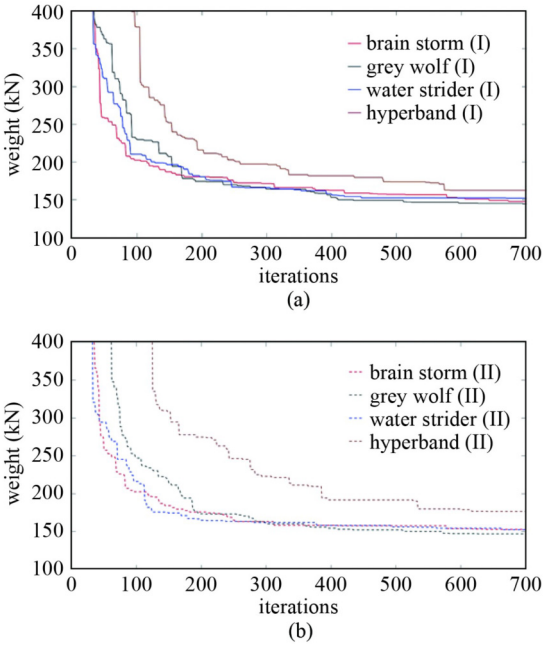

Fig. 10 Design history graphs for 354-bar spatial steel dome structure. (a) Without seismic load effect; (b) with seismic load effect.

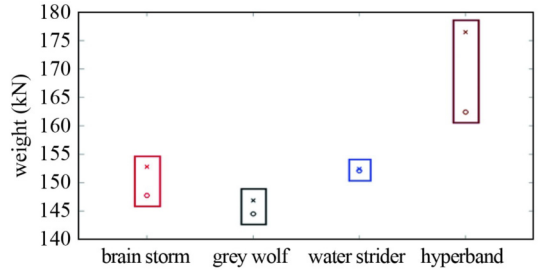

Fig. 11 The box plot of the optimum designs for 354-bar spatial steel dome structure. *o*: solutions without seismic effect, *x*: solutions with seismic effect.

dome designs with those previously reported using classical metaheuristic algorithms, a gradient descent-based HBO algorithm is executed. As design examples, three real size spatial steel dome structures are selected such as a 120-bar spatial steel dome structure, a 130-bar spatial steel dome structure, and a 354-bar spatial steel dome structure. In order to mutually transfer the data attained from the structural responses under external loadings, the open application interface (OAPI) functions are used to integrate the MATLAB with SAP2000. For all design examples both stress and stability constraints are executed by obeying the provisions of ASD-AISC practice code. Also, the maximum displacement constraints restricted the dome nodes. Additionally, in the second and the third design examples, slenderness ratio constraint is applied as stated in source studies to make a fair and accurate assessment. The tables and graphs are used to express the acquired optimal dome design in all design examples.

The main significant concluding remarks deducted from this study are summarized as follows.

1) In 120-bar spatial dome structure, for both load cases, with and without considering seismic effect, the GW algorithm designed a lighter dome compared to the classical HS, GA, and CO algorithms reported in the literature. Also, the optimally generated dome design via the GW algorithm is lighter than that generated by the newly proposed WS and BSO metaheuristic algorithms. The gradient descent-based HBO algorithm yielded the heaviest dome designs for both loading cases when compared with the proposed metaheuristic algorithms. In this design example, when the newly proposed WS and BSO algorithms are compared among themselves according to the load conditions, the WS algorithm achieves a better dome design in the load case where the seismic effect is not considered, while BSO algorithm achieves a better dome design in the load case where the seismic effect is considered. Although the seismic load effect caused an increase in structure weights obtained in optimum dome designs, this raise remained at the level of 0.12% for the BSO algorithm, 0.55% for the GW algorithm and 1.05% for the WS algorithm.

2) In the 130-bar spatial dome structure, the optimum dome designs obtained from GW and WS algorithms for both load cases with and without seismic load effect, and optimal dome design attained by BSO and HBO algorithms for load case without seismic load effect are exactly the same as that accomplished in previously reported source study. As a matter of fact, if the seismic load effect is considered in loading cases, the weights of dome designs achieved by BSO and HBO algorithms increased slightly by 0.83% and 4.55%, respectively, due to the change in the steel pipe section assigned to some element groups. These solutions reveal that the seismic load effect does not have a significant impact on optimal designs.

3) In 354-bar spatial dome structure, for the load case without considering seismic load effect, the GW algorithm achieved a second lighter dome compared to the classical metaheuristic algorithms reported in literature; while the optimum dome designed by GW algorithm is 0.18% lighter than that generated by the SA algorithm, it is 0.21% heavier than that resulted from the BB-BC algorithm. In this example, if the seismic effect is not considered in loading combinations, the BSO algorithm and the WS algorithm, respectively, generate slightly heavier dome designs than conventional algorithms. For this loading condition the gradient descent-based HBO algorithm yields the heaviest dome designs. Taking into consideration of the seismic load effect in loading condition, the GW algorithm obtained 3.78% and 4.05% lighter dome designs than those from the WS and BSO metaheuristic algorithms, respectively,

and obtained 20.13% lighter dome design than that of the HBO gradient descent-based algorithm. When the optimum dome designs are evaluated in terms of the proposed new algorithms, considering the seismic load effect in the loading, increments of 3.45%, 1.63%, 0.24%, and 8.64% are observed in the acquired dome design weights for the BSO, GW, WS, and HBO algorithms, respectively. These solutions clearly evince that the seismic load effect does have important impact upon the BSO metaheuristic algorithm, but has the highest effect on the gradient descent-based HBO algorithm.

4) In GW, WS, and BSO metaheuristic algorithms and HBO gradient descent-based algorithm for both load cases, despite the stress constraint acting as an important determinant on optimization process in first design example, the slenderness constraint dominates the optimum search process in the second and third design examples. But the displacement constraint does not show any impact on any of design examples. Also, in the third design example, the stress constraint has significant effect on optimization process in addition to slenderness constraint.

5) All the results ensure the pertinence and the validity of the proposed OAPI scheme leading reciprocal data interaction streaming between MATLAB and SAP2000 for seismic design optimization of spatial steel dome structures.

References

1. Makowski Z S. Braced domes, their history, modern trends and recent developments. Architectural Science Review, 1962, 5(2): 62−79
2. Makowski Z S. Analysis, Design, and Construction of Braced Domes. New York: Nichols Publishing Company, 1984
3. Manhor K, Annigeri A P. Analysis and comparing result of lamella dome and schwedler dome under application of external loads. International Journal of Innovative Science and Research Technology, 2019, 4(6): 206−209
4. Vazna R V, Zarrin M. Sensitivity analysis of double layer Diamatic dome space structure collapse behavior. Engineering Structures, 2020, 212: 110511
5. Guan Y, Virgin L N, Helm D. Structural behavior of shallow geodesic lattice domes. International Journal of Solids and Structures, 2018, 155: 225−239
6. Lebed E. Initial stress state at installation of a single-layer lattice dome due to errors of its assembly. IOP Conference Series: Materials Science and Engineering, 2020, 869(5): 052010
7. Zabojszcza P, Radoń U. The impact of node location imperfections on the reliability of single-layer steel domes. Applied Sciences (Basel, Switzerland), 2019, 9(13): 2742
8. Zabojszcza P, Radoń U, Obara P. Impact of single-layer dome modelling on the critical load capacity. MATEC Web of Conferences, 2018, 219: 02017
9. Binti Rosely N N A. Analysis of Structure Behaviour of Domes. Undergraduates Project Papers. Pahang: University Malaysia Pahang, 2015
10. Dede T, Grzywiński M, Selejdak J. Continuous size optimization of large-scale dome structures with dynamic constraints. Structural Engineering and Mechanics, 2020, 73: 397−405
11. Dede T, Grzywiński M, Venkata Rao R. Advances in Intelligent Systems and Computing. Berlin: Springer, 2020, 13−20
12. Lu M, Ye J. Guided genetic algorithm for dome optimization against instability with discrete variables. Journal of Constructional Steel Research, 2017, 139: 149−156
13. Grzywiński M, Dede T, Özdemír Y I. Optimization of the braced dome structures by using Jaya algorithm with frequency constraints. Steel and Composite Structures, 2019, 30: 47−55
14. Abu-Farsakh G, Al-Huthaifi N. Optimal aspect-ratio for various types of braced domes under gravity loads. Journal of Civil Engineering and Structures, 2018, 2(3): 1−7
15. Kaveh A, Javadi S M. Chaos-based firefly algorithms for optimization of cyclically large-size braced steel domes with multiple frequency constraints. Computers & Structures, 2019, 214: 28−39
16. Grzywiński M. Teaching-learning-based optimization algorithm for design of braced dome structures. In: Proceedings of XXIV LSCE Conference 2018. Lodz: Lodz University of Technology, 2018: 57−60
17. Kaveh A, Rezaei M. Optimum topology design of geometrically nonlinear suspended domes using ECBO. Structural Engineering and Mechanics: An international journal, 2015, 56(4): 667−694
18. Kaveh A, Rezaei M. Topology and geometry optimization of single-layer domes utilizing CBO and ECBO. Scientia Iranica, 2016, 23(2): 535−547
19. Kaveh A, Ilchi Ghazaan M. A new hybrid meta-heuristic algorithm for optimal design of large-scale dome structures. Engineering Optimization, 2018, 50(2): 235−252
20. Ye J, Lu M. Optimization of domes against instability. Steel and Composite Structures, 2018, 28: 427−438
21. Zhang H, Liang X, Gao Z, Zhu X. Seismic performance analysis of a large-scale single-layer lattice dome with a hybrid three-directional seismic isolation system. Engineering Structures, 2020, 214: 110627
22. Li Y G, Fan F, Hong H P. Reliability of lattice dome with and without the effect of using small number of ground motion records in seismic design. Engineering Structures, 2017, 151: 381−390
23. Kim Y-S, Kang J-W, Kim G-C. The seismic response analysis of lattice dome according to direction of seismic load. Journal of the Korean Association for Spatial Structures, 2018, 18(3): 133−140
24. Park K-G, Lee D-W. Reducing effect analysis on earthquake response of 100m spanned single-layered lattice domes with LRB seismic isolation system. Journal of the Korean Association for Spatial Structures, 2019, 19(1): 53−64
25. Park K-G, Chung M-J, Lee D-W. Earthquake response analysis for seismic isolation system of single layer lattice domes with 300m span. Journal of the Korean Association for Spatial Structures, 2018, 18(3): 105−116
26. Ding Y, Chen Z T, Zong L, Yan J B. A theoretical strut model for severe seismic analysis of single-layer reticulated domes. Journal of Constructional Steel Research, 2017, 128: 661−671

27. Yang D, Liu C Y, Hu M N, Zhang X. Seismic analysis of single-layer latticed domes composed of welded round pipes considering low cycle fatigue. International Journal of Structural Stability and Dynamics, 2017, 17(10): 1750122
28. Saleb I S, Muhsen T A. Dynamic response of braced domes under earthquake load. International Journal of Scientific and Engineering Research, 2018, 9: 29−39
29. Ooki Y, Kasai K, Motoyui S. Steel dome structure with viscoelastic dampers for seismic damage mitigation. In: Stessa 2003. Routledge, 2018, 641−648
30. Hosseinizad S A. Seismic response of lattice domes. Dissertation for the Doctoral Degree. Surrey: University of Surrey, 2018
31. AISC-ASD. Manual of Steel Construction: Allowable Stress Design, 1989
32. Kaveh A, Dadras Eslamlou A. Water strider algorithm: A new metaheuristic and applications. Structures, 2020, 25: 520−541
33. Mirjalili S, Mirjalili S M, Lewis A. Grey wolf optimizer. Advances in Engineering Software, 2014, 69: 46−61
34. Shi Y. Brain storm optimization algorithm. In: International Conference in Swarm Intelligence. Berlin: Springer, 2011
35. MATLAB. The Language of Technical Computing, 2009
36. SAP2000. Integrated Finite Element Analysis and Design of Structures, 2008
37. Carbas S, Toktas A, Ustun D. Nature-Inspired Metaheuristic Algorithms for Engineering Optimization Applications. 1st ed. Singapore: Springer Nature Singapore Pte. Ltd., 2021
38. Kaveh A, Ghazaan M I. Meta-heuristic Algorithms for Optimal Design of Real-size Structures. Cham: Springer International Publishing, 2018
39. Kaveh A. Applications of Metaheuristic Optimization Algorithms in Civil Engineering. Cham: Springer International Publishing, 2016
40. Yang X S. Nature-Inspired Algorithms and Applied Optimization. Cham: Springer International Publishing, 2018
41. Yang X S. Engineering Optimization: An Introduction with Metaheuristic Applications. New Jersey: John Wiley & Sons, Inc., 2010
42. Yang X S, Dey N, Fong S. Springer Tracts in Nature-Inspired Computing (STNIC). Cham: Springer Nature, 2020
43. Zhuang X, Guo H, Alajlan N, Zhu H, Rabczuk T. Deep autoencoder based energy method for the bending, vibration, and buckling analysis of Kirchhoff plates with transfer learning. European Journal of Mechanics-A/Solids, 2021, 87: 104225
44. Samaniego E, Anitescu C, Goswami S, Nguyen-Thanh V M, Guo H, Hamdia K, Zhuang X, Rabczuk T. An energy approach to the solution of partial differential equations in computational mechanics via machine learning: Concepts, implementation and applications. Computer Methods in Applied Mechanics and Engineering, 2020, 362: 112790
45. Anitescu C, Atroshchenko E, Alajlan N, Rabczuk T. Artificial neural network methods for the solution of second order boundary value problems. Computers, Materials and Continua, 2019, 59(1): 345−359
46. Guo H, Zhuang X, Rabczuk T. A deep collocation method for the bending analysis of Kirchhoff plate. Computers, Materials & Continua, 2019, 59(2): 433−456
47. Hamdia K M, Ghasemi H, Bazi Y, AlHichri H, Alajlan N, Rabczuk T. A novel deep learning based method for the computational material design of flexoelectric nanostructures with topology optimization. Finite Elements in Analysis and Design, 2019, 165: 21−30
48. Saremi S, Mirjalili S Z, Mirjalili S M. Evolutionary population dynamics and grey wolf optimizer. Neural Computing & Applications, 2015, 26(5): 1257−1263
49. Cheng S, Shi Y. Brain Storm Optimization Algorithms: Concepts, Principles and Applications. 1st ed. Cham: Springer International Publishing, 2019
50. Aldhafeeri A, Rahmat-Samii Y. Brain Storm Optimization for Electromagnetic Applications: Continuous and Discrete. IEEE Transactions on Antennas and Propagation, 2019, 67(4): 2710−2722
51. Cheng S, Qin Q, Chen J, Shi Y. Brain storm optimization algorithm: A review. Artificial Intelligence Review, 2016, 46(4): 445−458
52. Aydogdu I, Carbas S, Akin A. Effect of Levy Flight on the discrete optimum design of steel skeletal structures using metaheuristics. Steel and Composite Structures, 2017, 24(1): 93−112
53. American Association of State Highway and Transportation Officials (AASHTO). AASHTO LRFD Bridge Design Specifications. AASHTO, 2012
54. Lee K S, Geem Z W. A new structural optimization method based on the harmony search algorithm. Computers & Structures, 2004, 82(9−10): 781−798
55. Artar M. A comparative study on optimum design of multi-element truss structures. Steel and Composite Structures, 2016, 22(3): 521−535
56. Kaveh A, Ilchi Ghazaan M. Optimal design of dome truss structures with dynamic frequency constraints. Structural and Multidisciplinary Optimization, 2016, 53(3): 605−621
57. Hasancebi O, Erdal F, Saka M P. Optimum design of geodesic steel domes under code provisions using metaheuristic techniques. International Journal of Engineering and Applied Sciences, 2010, 2: 88−103
58. Hasançebi O, Çarbaş S, Doğan E, Erdal F, Saka M P. Performance evaluation of metaheuristic search techniques in the optimum design of real size pin jointed structures. Computers & Structures, 2009, 87(5−6): 284−302
59. Kaveh A, Talatahari S. A discrete Big Bang−Big Crunch algorithm for optimal design of skeletal structures. Asian Journal of Civil Engineering, 2010, 11: 103−122
60. Li L, Jamieson K, DeSalvo G, Rostamizadeh A, Talwalkar A. Hyperband: A novel bandit-based approach to hyperparameter optimization. Journal of Machine Learning Research, 2016, 18: 1−52
61. Soh C K, Yang J. Fuzzy controlled genetic algorithm search for shape optimization. Journal of Computing in Civil Engineering, 1996, 10(2): 143−150
62. ASCE/SEI 7-10. Minimum Design Loads for Buildings and Other Structures. Reston, VA: American Society of Civil Engineers, 2013